

TANTALOWODGINITE, $(\text{Mn}_{0.5}\square_{0.5})\text{TaTa}_2\text{O}_8$, A NEW MINERAL SPECIES FROM THE EMMONS PEGMATITE, UNCLE TOM MOUNTAIN, MAINE, U.S.A.

SARAH L. HANSON[§]

Geology Department, Adrian College, 110 S Madison St., Adrian, 49221 Michigan, U.S.A.

ALEXANDER U. FALSTER AND WILLIAM B “SKIP” SIMMONS

MP² Research Group, Maine Mineral and Gem Museum, PO Box 500, 99 Main St., Bethel, 04217 Maine, U.S.A.

RAYMOND SPRAGUE

10 Yates Street, Mechanic Falls, 04256 Maine, U.S.A.

PIETRO VIGNOLA

CNR-Istituto per la dinamica dei processi ambientali, via Mario Bianco, 9, I-20131 Milano, Italia

NICOLA ROTIROTI

Dipartimento di Scienze della Terra, Università degli Studi di Milano, via Botticelli 2, I-20133 Milano, Italia

SERGIO ANDÓ

Dipartimento di Scienze dell'Ambiente e del Territorio e di Scienze della Terra, Università Milano-Bicocca, Piazza della Scienza 4 - 20126 Milano, Italia

FRÉDÉRIC HATERT

Laboratoire de Minéralogie et Cristallogéologie, Département de Géologie, Université de Liège, Bâtiment B18, B-4000 Liège, Belgique

ABSTRACT

Tantalowodginite is a new mineral found in the Emmons granite pegmatite dike in Oxford County, Maine, U.S.A. It occurs as anhedral masses (0.5–12 cm) in the pegmatite core composed of K-feldspar, quartz, almandine, and schorl. Rarely, it occurs as crystals (0.2–1 cm) in miarolitic cavities associated with muscovite and fluorapatite. Tantalowodginite is rimmed with either black wodginite or columbite-(Mn). It is orange-red to deep red in color, semitransparent with a vitreous to sub-adamantine luster, has a yellowish-tan streak, is brittle with a conchoidal fracture, and shows a distinct {100} cleavage. The Mohs hardness is 5.5. Calculated density is 7.87 g/cm³ and the measured density is 7.61(1) g/cm³. Tantalowodginite is biaxial positive (+) and has a 2*V* angle of $\cong 70^\circ$ with strong dispersion. It exhibits weak to moderate pleochroism: orangish-yellow parallel to cleavage and greenish-yellow perpendicular to cleavage on (010). The measured *Z*∧*c* is 5–12°. The birefringence is strong to extreme; interference colors are very high-order tints in golden yellow. The refractive index (RI) is greater than 2.00 and the calculated mean RI is 2.24. Tantalowodginite is non-fluorescent under 254 nm (short wave) and 366 nm (long wave) ultraviolet light. The average chemical analysis of six electron microprobe analyses is Li₂O 0.54, MnO 6.23, FeO 0.23, TiO₂ 0.01, SnO₂ 8.14, Nb₂O₅ 3.97, Ta₂O₅ 80.75, total 99.88. The simplified formula is $(\text{Mn}_{0.5}\square_{0.5})\text{TaTa}_2\text{O}_8$. X-ray diffraction data show that tantalowodginite is monoclinic, space group *C2/c*. The refined unit-cell parameters are *a* 9.542(1) Å, *b* 11.488(2) Å, *c* 5.128(1) Å, and β 91.13(1)°, with *Z* = 4. In the wodginite structure there are three octahedrally coordinated sites. The A- and B-sites form zig-zag chains along *z* via edge sharing. Within these chains, the A- and B-sites alternate within the same plane. The

[§] Corresponding author e-mail address: slhanson@adrian.edu

C-sites form chains *via* edge sharing that lie in a different plane and connect the A-B chains by sharing apices alternately with the A and B polyhedra. The strongest measured X-ray powder diffraction lines are [d in Å, (I/I_0), (hkl): 7.332 (20) (110), 4.741 (20) (200), 3.838 (30) (021), 3.667 (100) (220), 3.000 (100) ($\bar{2}21$), 2.957 (100) (221), 2.883 (30) (040), and 1.778 (30) (260). The type specimen is deposited in the mineralogical collection of the Maine Mineral and Gem Museum, 99 Main Street, Bethel, Maine, U.S.A.

Keywords: tantalowodginite, wodginite group, new mineral species, EMPA, crystal structure, Emmons pegmatite, Oxford County, Maine.

INTRODUCTION

Wodginite ($\text{MnSnTa}_2\text{O}_8$) was introduced by Nickel *et al.* (1963) and was defined as a monoclinic mineral with space group $C2/c$ by Ferguson *et al.* (1976). Ercit *et al.* (1992b) noted that the chemistry of wodginite is more complex, as many of these minerals deviate from the ideal composition by more than 50% at the individual cation sites. These authors proposed that these minerals be given group status and be classified on the basis of the dominant cation at each of the individual sites. Ercit *et al.* (1992c) reported four wodginite mineral species including wodginite ($\text{MnSnTa}_2\text{O}_8$), ferrowodginite ($\text{Fe}^{2+}\text{SnTa}_2\text{O}_8$), titanowodginite ($\text{MnTiTa}_2\text{O}_8$), and lithiowodginite ($\text{LiTaTa}_2\text{O}_8$). More recently, ferrotitanowodginite ($\text{Fe}^{2+}\text{TiTa}_2\text{O}_8$) was described by Galliski *et al.* (1999). Ercit *et al.* (1992c) also reported “tantalowodginite” ($\text{Mn}_2\text{Ta}_4\text{Ta}_8\text{O}_{32}$), but later retracted that proposal, as the minute quantity of the sample precluded any measurement of Li or the X-ray properties of the sample.

Ideally, wodginite-group minerals are structurally ordered with cation occupancies as described above. However, Ercit *et al.* (1992a, b) showed that the degree of cation ordering for wodginite-group minerals is variable and that partially ordered samples are structurally intermediate to wodginite (completely ordered) and ixiolite (completely disordered). Distortion of the A, B, and C coordination octahedra are commensurate with the degree of disorder at these sites.

“Tantalowodginite” was identified from the Emmons pegmatite dike in Oxford County, Maine. The composition $(\text{Mn,Li})_4(\text{Ta,Sn})_4(\text{Ta,Nb})_8\text{O}_{32}$ was confirmed by electron microprobe analyses and the new mineral species was submitted for approval to the IMA in 2000 (IMA2000-26). However, the name was not approved pending a complete structural analysis. Subsequent crystal-structure determinations and X-ray powder diffraction analyses were completed using the same sample from which the chemical determinations were made. In this paper, we present the complete description of tantalowodginite, a new

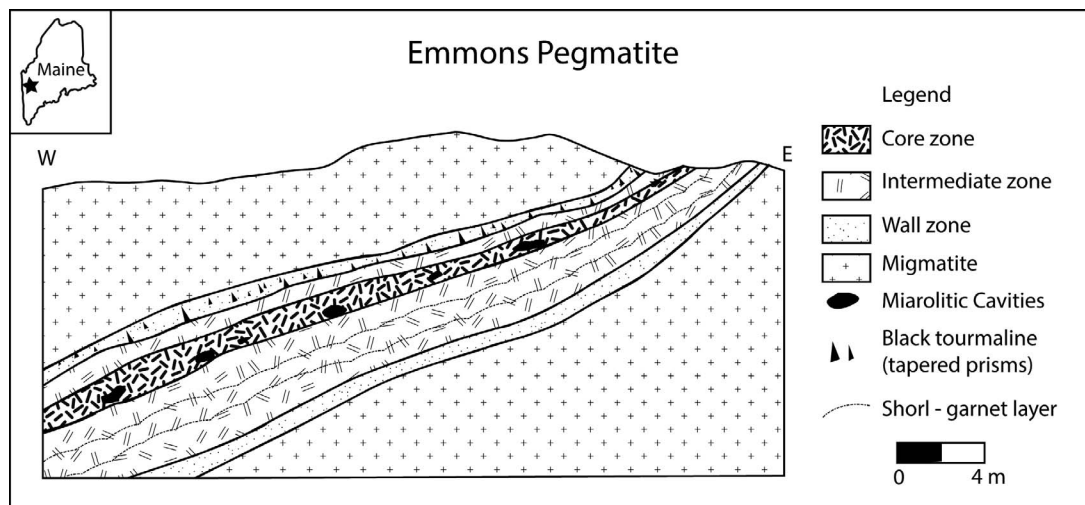


FIG. 1. Simplified cross-section of the Emmons Pegmatite (modified from Roda-Robles 2013).

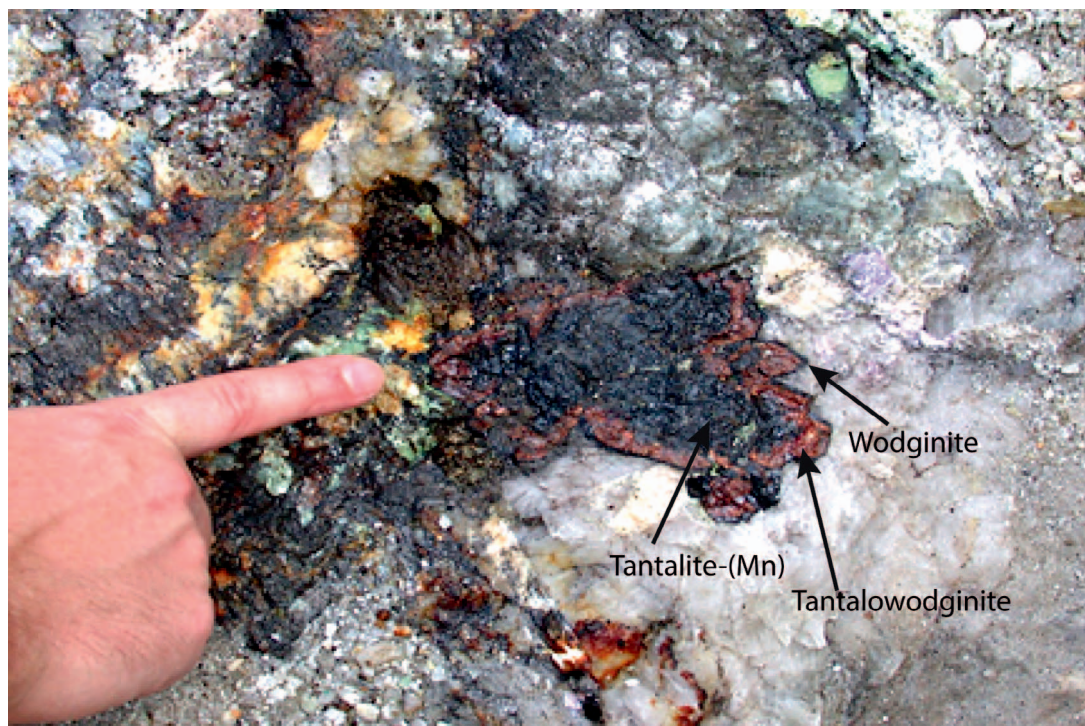


FIG. 2. Cross-section of a crystal cluster showing a tantalite-(Mn) core (black) with a tantalowodginite middle section (orange-red to deep red) and a wodginite rim (black) exposed in the Emmons pegmatite.

member of the wodginite group. The new species and its name have been approved by the IMA Commission on New Minerals, Nomenclature and Classification (IMA2017-095), and the notification and brief description is published in the *European Journal of Mineralogy* (Hanson *et al.* 2018).



FIG. 3. Tantalowodginite crystal overgrown with black columbite-(Mn), 12 cm wide. Currently housed at the Maine Mineral and Gem Museum.

OCCURRENCE

Tantalowodginite was found by one of the authors (RS) during mining activities in the Emmons pegmatite. The Emmons pegmatite is exposed on Uncle Tom Mountain near the town of Greenwood in Oxford Co., Maine, U.S.A (44°19'24.37" N, 70°41'45.02" W) and is part of the Oxford Pegmatite Field (Simmons *et al.* 2017). The pegmatite intruded a high-grade metasedimentary migmatitic sequence that shows plastic deformation. A simplified cross-section is shown in Figure 1. The comb-structure schorl is evidence of rapid crystallization of the pegmatite, likely the result of strong undercooling of the melt. Preliminary U-Pb dates of zircon give an age of about 250 Ma for the pegmatite (Roda-Robles *pers. commun.* 2017), which is consistent with recent dates of Oxford county pegmatites by Bradley *et al.* (2016).

The pegmatite is complexly zoned with a wall zone comprised of K-feldspar, quartz, almandine, and schorl, which locally exhibits a well-developed comb structure. The intermediate zones are comprised of K-feldspar, quartz, muscovite, and altered spodumene. A quartz-rich core is present but is poorly exposed. Replacement units along the core-intermediate zone

TABLE 1. COMPARISON OF THE PHYSICAL PROPERTIES OF MINERALS BELONGING TO THE WODGINITE GROUP

Mineral Reference	wodginite [1, 2]	ferrowodginite [2]	titanowodginite [2]	ferrotitanowodginite [3]	lithiowodginite [4]	tantalowodginite This work
Ideal formula*	$\text{Mr}^{2+}\text{Sn}^{4+}\text{Ta}_2\text{O}_8$	$\text{Fe}^{2+}\text{Sn}^{4+}\text{Ta}_2\text{O}_8$	$\text{Mr}^{2+}\text{TiTa}_2\text{O}_8$	$\text{Fe}^{2+}\text{TiTa}_2\text{O}_8$	LiTa_3O_8	$(\text{Mn}_{0.5}\square_{0.5})\text{TaTa}_2\text{O}_8$
Space group	C2/c or Cc	C2/c	C2/c	C2/c	C2/c	C2/c
a (Å)	9.52	9.415 (7)	9.466 (2)	9.403 (4)	9.441 (3)	9.542 (1)
b (Å)	11.46	11.442 (6)	11.431 (1)	11.384 (3)	11.516 (4)	11.488 (2)
c (Å)	5.11	5.103 (4)	5.126 (1)	5.075 (1)	5.062 (2)	5.128 (1)
β (°)	91.15	90.8 (1)	90.31 (2)	90.55 (2)	91.06	91.13 (1)
Z	4	4	4	4	4	4
Strong X-ray lines	7.22 (11) 4.76 (11)	—	—	7.230 (10) 4.693 (20)	—	7.332 (20) 4.741 (20)
	3.67 (70) 3.00 (100)	3.64 (20) 2.97 (100)	3.644 (46) 2.976 (100)	3.790 (20) 2.963 (100)	3.65 (82) 2.987 (100)	3.667 (100) 3.000 (100)
	2.95 (70)	—	2.966 (95)	2.939 (90)	2.940 (50)	2.957 (100)
	2.87 (25)	2.86 (20)	2.858 (15)	2.849 (25)	—	2.883 (30)
	2.55 (21)	2.55 (30)	2.563 (15)	2.539 (30)	2.502 (38)	2.560 (20)
	2.50 (29)	2.493 (40)	2.495 (36)	2.484 (45)	—	2.511 (20)
	2.38 (10)	2.352 (20)	—	2.350 (15)	—	2.380 (20)
	1.831 (14)	—	—	1.812 (15)	—	1.834 (20)
	1.774 (27)	—	—	—	—	1.778 (30)
	1.760 (13)	1.768 (20)	1.767 (17)	1.759 (45)	—	1.761 (20)
Cleavage	—	—	—	none	—	{110}
Density	7.36–7.19 meas. 7.69–7.81 calc.	7.02 calc.	6.86(3) meas. 6.89 calc.	7.368 calc.	7.5 (2) meas. 7.74 (1) calc.	7.61 meas. 7.87 calc.
Optical sign	—	+	+	—	—	+
2V (°)	—	—	—	—	—	70°
Hardness	—	5.5 (Mohs)	5.5 (Mohs)	5.5 (Mohs)	5–6 (Mohs)	5.5 (Mohs)
Color	Reddish-brown to black	Dark brown to black	Dark brown to black	Very dark brown-black	Dark pink to red	Orange, orange red to deep red

[1] Nickel *et al.* (1963), [2] Ercit *et al.* (1992c), [3] Galliski *et al.* (1999), [4] Voloshin *et al.* (1990), * formulas from IMA master list.

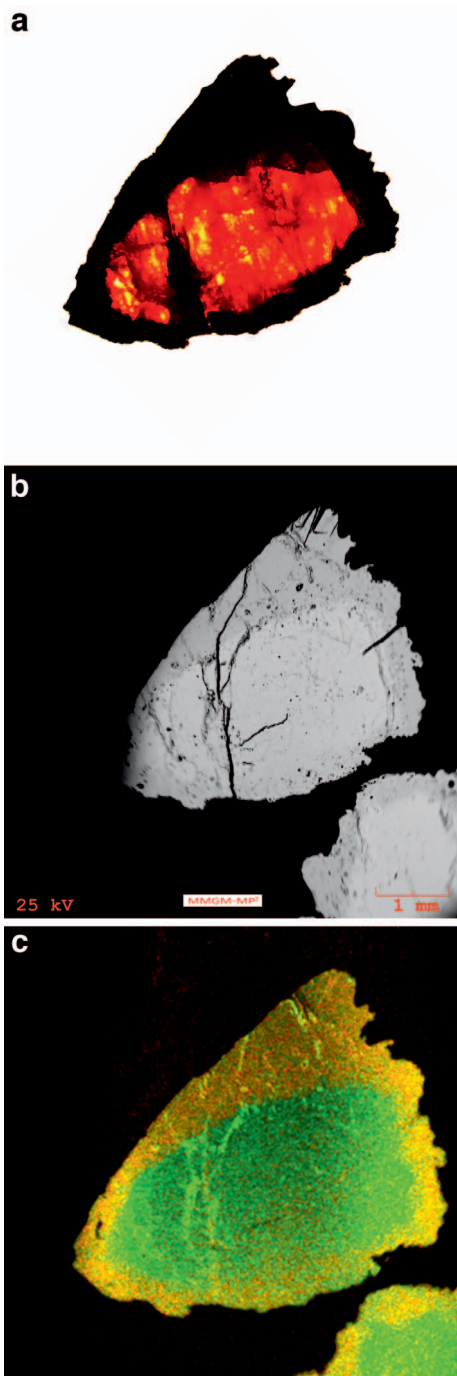


Fig. 4. Sliced crystal showing (a) tantalowodginite core (orange-red) with wodginite overgrowth (black). (b) SEM backscattered electron image. (c) Composite SEM X-ray map: red (Mn) and green (Ta).

boundary have undergone almost total alteration and replacement such that the only primary mineral remaining is muscovite. Secondary minerals include vuggy albite, cleavelandite, and a dense and fibrous grayish-green muscovite that occurs as a fracture filling and as a secondary mineral replacing schorl and garnet. Additionally, pollucite pods several meters in size, large phosphate nodules (up to 15 cm in diameter), löllingite with minor arsenopyrite, and nearly gem-quality beryl (aquamarine, morganite, and goshenite) crystals up to 30 cm in size are present.

GENERAL APPEARANCE AND PHYSICAL PROPERTIES

In the quartz–K-feldspar pegmatite core, tantalowodginite forms primary anhedral masses or clusters of masses that are rimmed by wodginite, with both sometimes occurring as rims on tantalite-(Mn) cores (0.5–12 cm; Fig. 2). Rarely it can be found in miarolitic cavities as crystals (0.2–1 cm) of tantalowodginite that are rimmed by columbite-(Mn) (Fig. 3). These crystals are typically associated with muscovite and fluorapatite. A comparison of the appearance and properties of tantalowodginite with other wodginite-group species is given in Table 1. Tantalowodginite is orange-red to deep red in color, semitransparent with a vitreous to sub-adamantine luster, and has a yellowish-tan streak. The mineral is brittle with a conchoidal fracture and shows a distinct {100} cleavage. Its Mohs hardness is 5.5. The density, calculated from the formula weight (from the averaged microprobe analysis) and single crystal unit-cell parameters (volume), is 7.87 g/cm³, which agrees well with the density measured by means of Berman balance, 7.61(1) g/cm³. The mineral is biaxial positive (+) and the refractive index (RI) was determined by immersion oils to be greater than 2.00. The calculated mean RI is 2.24 by the Gladstone-Dale relationship. The measured $2V$ angle is $\cong 70^\circ$ with a strong dispersion. The pleochroism is weak to medium: orangish-yellow parallel to cleavage, and greenish-yellow perpendicular to cleavage on (010). The measured $Z \wedge c$ is 5–12°. The birefringence is strong to extreme; interference colors are very high-order tints of golden yellow. Due to strong dispersion, the colors often change to anomalously sky blue, which appears only close to the extinction point. In these crystals the interference figure displays a typical feature with an isogyre on the edge of the optical field, similar to $C2/c$ clinopyroxenes. Tantalowodginite is non-fluorescent under 254 nm (short wave) and 366 nm (long wave) ultraviolet light. The type sample used for the complete characterization of the new species tantalowodginite is deposited in the mineralogical collection of the Maine Mineral and Gem

TABLE 2. REPRESENTATIVE COMPOSITIONS OF TANTALOWODGINITE AND WODGINITE FROM THE EMMONS PEGMATITE

	Tantalowodginite				Wodginite		
	TW1-4	TW1-20	TW2-9	TW2-24	Wod-2	Wod-27	Wod-28
MnO	6.15	6.08	5.92	5.67	10.08	9.29	9.51
FeO	0.206	0.129	0.073	0.264	1.208	1.858	1.856
SnO ₂	8.45	8.83	8.86	8.84	16.65	16.86	15.82
TiO ₂	0.000	0.052	0.000	0.000	0.354	0.053	0.540
Ta ₂ O ₅	80.72	80.49	80.62	81.02	69.12	69.24	69.32
Nb ₂ O ₅	3.48	3.67	4.11	3.91	3.99	2.80	3.86
Li ₂ O	0.510	0.510	0.586	0.586	0.054	0.054	0.054
Total	99.006	99.305	99.594	99.700	101.425	100.108	100.916
A-site							
Mn	0.579	0.570	0.552	0.528	0.911	0.858	0.864
Fe ²⁺	0.019	0.012	0.007	0.024	0.108	0.170	0.166
Li	0.228	0.227	0.259	0.259	0.023	0.024	0.023
Vacancy	0.174	0.191	0.183	0.188			
Sum	1.000	1.000	1.000	1.000	1.042	1.052	1.053
B-site							
Sn	0.375	0.390	0.388	0.387	0.708	0.733	0.676
Ti	0.000	0.004	0.000	0.000	0.028	0.004	0.044
Ta	0.615	0.606	0.614	0.617	0.198	0.193	0.207
Sum	0.990	1.000	1.002	1.005	0.936	0.932	0.927
C-site							
Nb	0.175	0.184	0.204	0.194	0.193	0.138	0.187
Ta	1.825	1.816	1.796	1.806	1.807	1.862	1.813
Sum	2.000	2.000	2.000	2.000	2.000	2.000	2.000

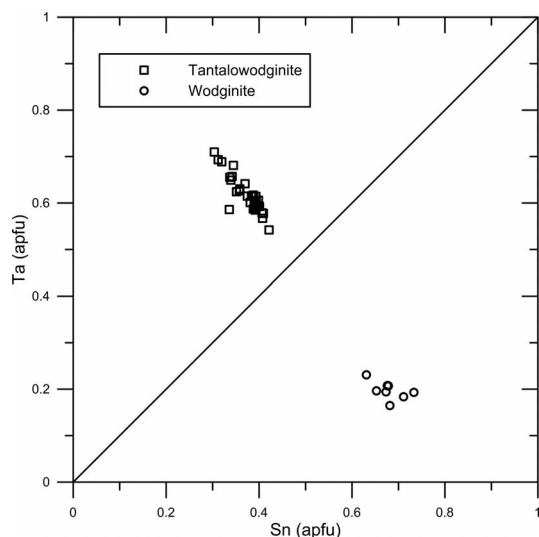


FIG. 5. B-site composition of tantalowodginite and wodginite.

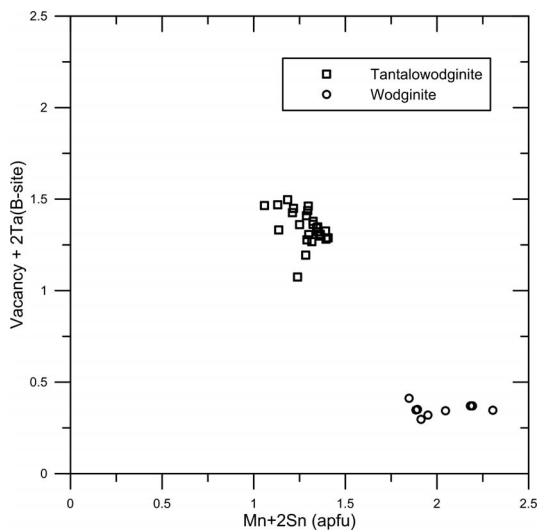
FIG. 6. Graphical representation of the substitution equation $(^A\Box\ ^B[Ta^{5+}]_2 = ^A[Mn^{2+}]_{-1}\ ^B[Sn^{4+}]_{-2})$ for the formation of tantalowodginite, from Ercit *et al.* (1992c).

TABLE 3. REPRESENTATIVE CHEMICAL COMPOSITION OF TANTALITE-(Mn) FROM THE EMMONS PEGMATITE

	T-1	T-2	T-3	T-4	T-5
MnO	12.44	12.65	11.15	12.90	12.67
FeO	2.28	1.90	3.55	1.66	1.89
TiO ₂	0.03	0.03	0.01	0.01	0.00
SnO ₂	0.21	0.23	0.11	0.09	0.15
Nb ₂ O ₅	8.80	7.12	6.64	7.34	7.57
Ta ₂ O ₅	76.38	77.85	78.57	78.05	77.67
Total	100.15	99.78	100.03	100.05	99.94
A-site					
Mn ²⁺	0.848	0.875	0.772	0.889	0.873
Fe ²⁺	0.154	0.130	0.243	0.113	0.129
Sum	1.002	1.005	1.015	1.002	1.002
B-site					
Sn	0.007	0.008	0.004	0.003	0.005
Ti	0.002	0.002	0.001	0.000	0.000
Ta	1.672	1.728	1.746	1.726	1.718
Nb	0.320	0.263	0.245	0.270	0.278
Sum	2.001	2.001	1.996	2.000	2.001

Museum, 99 Main Street, Bethel, Maine, U.S.A. (catalogue number MMGM-MP²-12-10-2016).

CHEMICAL COMPOSITION

Quantitative chemical analyses were obtained from polished carbon-coated sections of tantalowodginite using a CAMECA SX-50 electron microprobe working in wavelength-dispersion mode at the University of Utah. The system was operated using an accelerating voltage of 15 kV, a beam current of 30 nA, a spot size of 3 μm, and a counting time of 30 s on the peaks and 10 s on the backgrounds. The following minerals were used as standards: tantalite-(Mn) (Alto do Giz) for Ta and Mn, hematite (Elba) for Fe, synthetic rutile for Ti, and synthetic cassiterite for Sn. Synthetic Y-niobate was used to calibrate Nb. Matrix effects were corrected using the $\phi(\rho Z)$ correction procedure (Pouchou & Pichoir 1991). Lithium content was measured from two tantalowodginite samples and one wodginite sample. Pulverized samples were dried overnight in a drying oven, weighed, and digested in a flux of potassium bisulfate in a platinum crucible for 15 min. The cooled flux cake was dissolved in diluted sulfuric acid and analyzed with a Beckman Spectrascan V DCP using Li-nitrate standard solutions.

Both wodginite and tantalowodginite from the Emmons Quarry exhibit little chemical variation within each phase and the boundaries between the two phases are abrupt (Fig. 4a–c). Representative electron microprobe compositions are given for

tantalowodginite and wodginite in Table 2. For wodginite-group minerals, site occupancies are such that Mn, Li, Fe, and vacancies occupy the A-site; Ta, Ti, and Sn the B-site; and Nb and Ta the C-site. Wodginite group minerals are dominated by Ta at the C-site. The A-site for both wodginite and tantalowodginite is populated predominantly by Sn. Tantalowodginite exhibits greater Li substitution at the B-site, whereas the wodginite contains more Fe²⁺. The B-site occupancy differentiates the two minerals, as Ta is dominant in tantalowodginite and Sn in wodginite overgrowths. This distinct separation of the B-site occupancy is illustrated in Figure 5. This plot also reveals a nearly one-to-one ratio of the elements, suggesting this substitution is proportional to the primary substitution mechanism for wodginite and tantalowodginite. However, for this to be the case a coupled substitution must exist to maintain charge neutrality. Ercit *et al.* (1992c) proposed the following coupled substitution equation for the formation of these two minerals:



This substitution operator was evaluated by calculating Li for the remainder of the electron microprobe analyses using the FORTRAN program of Ercit *et al.* (1992b) and plotting the data on a diagram with ^AMn + 2^BSn on the X axis and A-site vacancies + 2^BTa on the Y axis (Fig. 6). The near one-to-one ratio implies that

TABLE 4. THE X-RAY POWDER DIFFRACTION PATTERN OF TANTALOWODGINITE (*d* in Å)

<i>l</i> / <i>h</i>	<i>d</i> _{obs}	<i>d</i> _{calc}	<i>h k l</i>
20	7.332	7.333	110
10	5.761	5.760	020
20	4.741	4.754	200
10	4.230	4.229	111
10	4.162	4.164	111
30	3.838	3.825	021
100	3.667	3.666	220
100	3.000	3.004	221
100	2.957	2.957	221
30	2.883	2.880	040
10	2.650	2.648	311
20	2.560	2.558	002
20	2.511	2.510	041
10	2.469	2.463	240,330
10	2.402	2.403	112
20	2.380	2.377	400
10	2.213	2.210	241
10	2.114	2.114	222
10	2.081	2.082	222
10	2.002	2.004	421
10	1.913	1.912	042
20	1.834	1.833	440
30	1.778	1.780	260
20	1.761	1.760	402
10	1.752	1.753	332

this is the predominant operator for B-site substitution in wodginite and tantalowodginite.

For tantalowodginite, an average empirical formula, calculated on the basis of 8 oxygen atoms per formula unit, is (Mn_{0.58}Li_{0.24}Fe_{0.02}□_{0.16})Σ_{1.00}(Ta_{0.62}Sn_{0.36}Ti_{0.01})Σ_{0.99}(Ta_{1.83}Nb_{0.17})Σ_{2.00}O₈. The simplified formula is (Mn_{0.5}□_{0.5})TaTa₂O₈, which theoretically requires MnO 5.08 wt.% (with Mn = 0.5 *apfu*) and Ta₂O₅ 94.92 wt.%, for a total of 100.00 wt.%.

Tantalite-(Mn) is present as cores in some of the wodginite crystals. Analyses are given in Table 3 and reveal a similar chemical composition, as Sn is dominant at the A-site and Ta at the B-site.

X-RAY DIFFRACTION DATA AND CRYSTAL STRUCTURE REFINEMENT

The X-ray powder diffraction pattern of tantalowodginite was recorded using a Scintag XDS-2000 X-ray diffractometer, CuKα radiation (1.5406 Å). Operating conditions were 35 kV, 15 nA. Unit-cell parameters were refined from XRD powder data, starting from the unit-cell parameters described for wodginite and using the software CELL (Appleman &

TABLE 5. DETAILS PERTAINING TO THE DATA COLLECTION AND STRUCTURE REFINEMENT OF TANTALOWODGINITE

Crystal shape	Irregular prism
Crystal size (μm)	50 × 75 × 115
Crystal color	Orange red to deep red
<i>T</i> (K)	298
Unit-cell constants	<i>a</i> = 9.542 (1) Å <i>b</i> = 11.488 (2) Å <i>c</i> = 5.128 (1) Å <i>β</i> = 91.13 (1) ° <i>V</i> = 562.1 (2) Å ³
Reference chemical formula	Mn _{0.5} □ _{0.5} TaTa ₂ O ₈
Space Group	C2/ <i>c</i>
<i>Z</i>	4
Radiation	MoKα
<i>h</i> _{min} , <i>h</i> _{max}	-13, 13
<i>k</i> _{min} , <i>k</i> _{max}	-17, 16
<i>l</i> _{min} , <i>l</i> _{max}	-8, 8
Redundancy	6.9
Measured reflections	7168
Unique reflections	1034
Unique refl. with <i>I</i> > 3σ(<i>I</i>)	762
Parameters (refinement)	40
<i>R</i> _{int} (obs/all)(%)	5.90/6.17
<i>R</i> ₁ (obs/all)(%)	2.73/5.12
Final <i>wR</i> ₂	2.44/2.91
Residuals (e ⁻ / Å ³)	+2.99/-2.88

$$R_{\text{int}} = \frac{\sum |F_{\text{obs}}^2 - F_{\text{obs}}^2(\text{mean})|}{\sum F_{\text{obs}}^2}; R_1 = \frac{\sum (|F_{\text{obs}} - F_{\text{calc}}|)}{\sum F_{\text{obs}}}; wR2 = \frac{(\sum (w(F_{\text{obs}}^2 - F_{\text{calc}}^2)^2))^{0.5}}{\sum (w(F_{\text{obs}}^2)^{0.5})}; w = 1/(\sigma^2(F_{\text{obs}}^2))$$

Evans 1973). The powder pattern reflections were found to be consistent with the space group C2/*c*. The complete list of indexed reflections is reported in Table 4. The eight strongest measured lines are [*d* in Å, (*l*/*h*), (*hkl*)]: 7.332 (20) (110), 4.741 (20) (200), 3.838 (30) (021), 3.667 (100) (220), 3.000 (100) (221), 2.957 (100) (221), 2.883 (30) (040), and 1.778 (30) (260). The refined unit-cell parameters are *a* 9.510(6) Å, *b* 11.520(6) Å, *c* 5.118(3) Å, *β* = 91.22(5)°, and *V* 560.6 (3) Å³ for *Z* = 4.

Intensity data for a 0.05 × 0.075 × 0.115 mm single crystal of tantalowodginite were collected using an Agilent Xcalibur 4-circle diffractometer equipped with an EOS CCD detector at the Earth Science Department, University of Milano by phi and omega rotation. The data were first processed with the CrysAlis software for absorption and Lorentz-Polarization corrections. Details pertaining to the data collection and structure refinement are summarized in Table 5. The unit-cell parameters are *a* 9.542(1) Å, *b* 11.488(2) Å, *c* 5.128(1) Å, and *β* 91.13(1)°, with *Z* = 4. Space group tests led to the C2/*c* space group. The crystal

TABLE 6. REFINED POSITIONAL AND DISPLACEMENT PARAMETERS (\AA^2) FOR TANTALOWODGINITE

	Element	Occ	x	y	z	U_{iso}
A	Mn	0.971(14)	0	0.65583(15)	0.25	0.0064(5)
B	Ta	0.651(8)	0	0.16878(7)	0.25	0.00577(18)
C	Ta	0.912(10)	0.24982(4)	0.41284(3)	0.24692(7)	0.00439(8)
O1	O	1	0.1358(5)	0.0574(4)	0.0775(9)	0.0051(11)
O2	O	1	0.1466(5)	0.4514(5)	0.5567(10)	0.0083(11)
O3	O	1	0.1204(5)	0.3057(5)	0.1035(9)	0.0077(11)
O4	O	1	0.1163(5)	0.1866(5)	0.5879(9)	0.0068(11)

structure of tantalowodginite was solved by the SUPERFLIP program (based on the charge flipping algorithm, Palatinus & Chapuis 2007), implemented in JANA2006 (Petricek *et al.* 2014), on the basis of intensity data collected using MoK α monochromatic radiation (0.71039 \AA). The atomic positions (Table 6) were found to be in good agreement with those described by Ercit *et al.* (1992a) for minerals belonging to the wodginite group. The refinement was finalized using anisotropic displacement parameters for Mn at A- and Ta at B- and C-sites and isotropic displacement parameters for oxygen atoms. All attempts to anisotropically refine the oxygen atoms did not give any improvement in the crystal-structure refinement. Moreover, all values of anisotropic thermal displacement parameters were close to their standard deviation, thus were not meaningful. Specifically, the U_{eq} parameter for O1 was slightly negative. When convergence was achieved, no peak larger than +2.99 and $-2.88 \text{ e}^{-}/\text{\AA}^3$ was present in the final

difference-Fourier map. Such peaks were mainly located close to the A- and B-sites (probably due to the structural disorder, see below). Selected bond distances for tantalowodginite are reported in Table 7. The general structure of tantalowodginite conforms to that described in Ferguson *et al.* (1976) and Ercit *et al.* (1992a). In the wodginite structure there are three different cation sites as described above. All cations are in octahedral coordination. The A and B octahedra form zig-zag chains along *z* via edge sharing. Within these chains, the A- and B-sites alternate within the same plane. The C-sites form chains *via* edge sharing that lie in a different plane and connect the A-B chains by sharing apexes alternately with the A and B polyhedra (Fig. 7). A comparison of the distribution of metals in the chemical analysis, $(\text{Mn}_{0.58}\text{Li}_{0.24}\text{Fe}_{0.02}\square_{0.16})\Sigma_1(\text{Ta}_{0.62}\text{Sn}_{0.36})\Sigma_{0.98}(\text{Ta}_{1.80}\text{Nb}_{0.20})_2\text{O}_8$, in terms of electrons, with that inferred from the structure refinement is shown in Table 8. From the table it is evident that the C-site is almost completely ordered

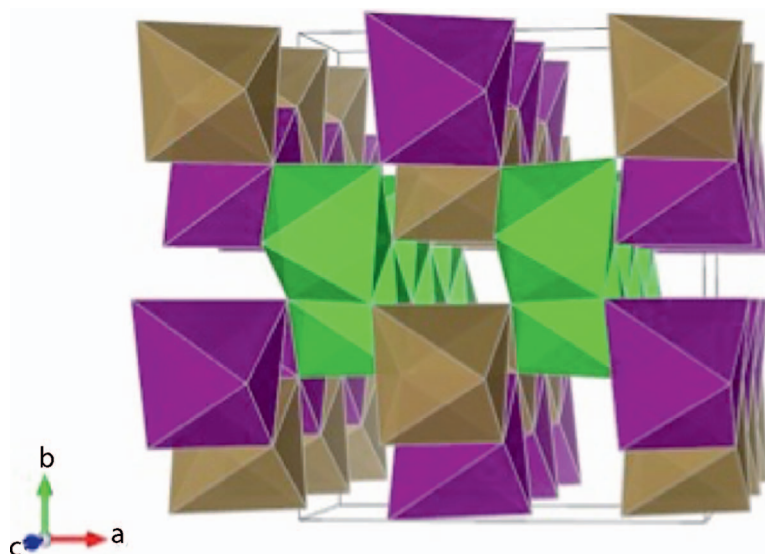


Fig. 7. Crystal structure of tantalowodginite: A-site is purple, B-site brown, C-site green.

TABLE 7. SELECTED BOND DISTANCES (Å) FOR TANTALOWODGINITE

A–O2 (b, c)	2.125 (5)	×2	C–O1 (g)	2.173(5)
A–O3 (d, e)	2.173 (5)	×2	C–O1 (h)	2.037(5)
A–O4 (b, c)	2.288 (6)	×2	C–O2 (a)	1.937(5)
<A–O>	2.195		C–O2 (c)	2.077(5)
			C–O3 (a)	1.883(5)
B–O1 (a, f)	2.036(5)	×2	C–O4 (i)	1.900(5)
B–O3 (a, f)	2.095(5)	×2	<C–O>	2.001
B–O4 (a, f)	2.050(4)	×2		
<B–O>	2.060			

Notes: a (x, y, z); b (–x, –y+1, –z+1); c (x, –y+1, z–1/2); d (–x, –y+1, –z); e (x, –y+1, z+1/2); f (–x, y, –z+1/2); g (–x+1/2, y+1/2, –z+1/2); h (–x+1/2, –y+1/2, –z); i (–x+1/2, –t+1/2, –z+1).

and occupied mainly by Ta. The electron distributions at A- and B-sites inferred from the crystal structure are different from those indicated by the chemical analyses. We ascribe this difference to strong cation disorder. For example, the gap may be balanced by moving a fraction of Li to the B-site and some Ta or Sn to the A-site. Nevertheless, the A-site is occupied predominantly by Mn and the B-site remains dominated by Ta, as proposed by the general formula for tantalowodginite. Table 9 shows the bond valences calculated for tantalowodginite.

DISCUSSION

Tantalowodginite is the Mn and Ta endmember in the wodginite group (Dana classification: 8.1.8.1, multiple oxides containing niobium, tantalum, or titanium; Nickel-Strunz classification: 4.DB.40, oxides D with medium-sized cations).

Both wodginite and tantalowodginite are present in the core of the Emmons pegmatite with the former occurring as thin overgrowths on the latter. Some of these wodginite/tantalowodginite pairs occur as

TABLE 8. COMPARISON OF e⁻ NUMBER AT A-, B-, AND C-SITES AS OBTAINED BY STOICHIOMETRY AND STRUCTURE REFINEMENT

Site	Chemical analysis (e ⁻)	Structure refinement (e ⁻)	Difference (%)
A	15.14	24.3	38
B	63.49	47.45	-25
A+B	78.63	71.75	9
C	140.56	133.15	5

Note: The number of electrons in the C-site takes into account site multiplicity (i.e., it is 2× the actual number of electrons in the C-site)

TABLE 9. BOND-VALENCE CALCULATION FOR TANTALOWODGINITE

	A	B	C	Σ
O1		0.754 (×2)	0.521	2.14
			0.752	
O2	0.363 (×2)		0.986	2.21
			0.675	
O3	0.319 (×2)	0.643 (×2)	1.141	2.49
O4	0.234 (×2)	0.726 (×2)	1.090	2.39
Σ	1.832	4.246	5.165	

overgrowths on tantalite-(Mn). Tantalowodginite results primarily from an increased substitution of Sn for Ta at the B-site. Charge balance necessitates a coupled substitution where two B-site Sn and one A-site Mn atoms substitute for two Ta atoms and create a vacancy at the A-site (Ericit *et al.* 1992c). Lack of zoning within the individual phases, coupled with abrupt transitions between the columbite-group minerals, tantalowodginite, and wodginite, suggests that these minerals did not result from continued fractionation as a magma composition slowly changed. Instead, they are attributed to several phases of crystallization within the core of the pegmatite. Initially, Sn abundance was likely low, as the early crystallizing Nb-Ta oxide was tantalite-(Mn), with virtually no substitution of Sn for Ta at the B-site. A subsequent increase in Sn activity, and perhaps Li, led to the formation of rims of tantalowodginite that encapsulate the tantalite-(Mn) masses. During the later stages of core formation, continued fractionation and commensurate increases in Sn abundance led to a third phase of crystallization of Nb-Ta-oxide minerals that resulted in the growth of a thin rind of wodginite on the tantalite-(Mn)/tantalowodginite masses. In contrast, tantalowodginite that forms in miarolitic cavities is overgrown by columbite-group minerals. The relative timing of the crystallization of these two overgrowth types cannot be determined.

ACKNOWLEDGMENTS

The first author would like to thank BP Nash for allowing me to use the electron microprobe at the University of Utah and for help with the analyses. We would also like to thank Pavel Uher and Daniel Atencio for helpful reviews that greatly improved the manuscript.

REFERENCES

APPLEMAN, D.E. & EVANS, H.T., JR. (1973) Job 9214: Indexing and least-squares refinement of powder diffraction data.

United States Geological Survey Computer Contributions **20** (NTIS Doc. PB2-16188).

- BRADLEY, D., SHEA, E., BUCHWALDT, R., BOWRING, S., BENOWITZ, J., O'SULLIVAN, P., & McCAULY, A. (2016) Geochronology and tectonic context of lithium-cesium-tantalum pegmatites in the Appalachians. *Canadian Mineralogist* **54**, 945–969.
- ERCIT, T.S., HAWTHORNE, F.C., & ČERNÝ, P. (1992a) The wodginite group. I. Structural Crystallography. *Canadian Mineralogist* **30**, 597–611.
- ERCIT, T.S., CERNY, P., HAWTHORNE, F.C., & McCAMMON, C.A. (1992b) The wodginite group. II. Crystal chemistry. *Canadian Mineralogist* **30**, 613–631.
- ERCIT, T.S., ČERNÝ, P., & HAWTHORNE, F.C. (1992c) The wodginite group. III. Classification and new species. *Canadian Mineralogist* **30**, 633–638.
- FERGUSON, R.B., HAWTHORNE, F.C., & GRICE, J.D. (1976) The crystal structures of tantalite, ixiolite and wodginite from Bernic Lake, Manitoba: II wodginite. *Canadian Mineralogist* **14**, 550–560.
- GALLISKI, M.A., ČERNÝ, P., MÁRQUEZ-ZAVALÍA, M.F., & CHAPMAN, R. (1999) Ferrotitanowodginite, $\text{Fe}^{2+}\text{TiTa}_2\text{O}_8$, a new mineral of the wodginite group from the San Elías pegmatite, San Luis, Argentina. *American Mineralogist* **84**, 773–777.
- HANSON, S.L., FALSTER, A.U., SIMMONS, W.B., SPRAGUE, R., VIGNOLA, P., ROTIROTI, N., ANDÓ, S., & HATERT, F. (2018) Tantalowodginite, IMA 2017-095. CNMNC Newsletter No. 41, February 2018, page 185; *European Journal of Mineralogy* **30**, 183–186.
- NICKEL, E.H., ROWLAND, J.F., & McADAM, R.C. (1963) Wodginite – a new tin-manganese tantalite from Wodgina, Australia and Bernic Lake, Manitoba. *Canadian Mineralogist* **7**, 390–402.
- PALATINUS, L. & CHAPUIS, B. (2007) SUPERFLIP – a computer program for the solution of crystal structures by charge flipping in arbitrary dimensions. *Journal of Applied Crystallography* **40**, 786–790.
- PETRICEK, V., DUSEK, M., & PALATINUS, L. (2014) Crystallographic Computing System JANA2006: General Features. *Zeitschrift für Kristallographie* **229**, 345–352.
- POUCHOU, J.L. & PICOIR, F. (1991) Quantitative analysis of homogenous or stratified microvolumes applying the model “PAP”. In *Electron probe quantitation* (K.F.J. Heinrich & D.E. Newbury, eds.). Plenum, New York (31–75).
- RODA-ROBLES, E. (2013) *PEG2013 Field Trip Guide Book*. PEG 2013, 6th International Symposium on Granite Pegmatites. 26 May–2 June 2013. Bartlett, New Hampshire. 62 pp.
- SIMMONS, W.B., FALSTER, A.U., WEBBER, K.L., FELCH, M.M., BRADLEY, D.C., RODA-ROBLES, E., FREEMAN, G., MORRISON, J., & NIZAMOFF, J.W. (2017) Lithium-Boron-Beryllium Gem Pegmatites, Oxford Co., Maine: Havey and Mount Mica Pegmatites. New England Intercollegiate Geological Conference at Maine Mineral and Gem Museum, Bethel, Maine, United States, 34 pp.
- VOLOSHIN, A.V., PAKHOMOVSKII, YA.A., & BAKHCHISARAITSEV, A.YU. (1990) Lithiowodginite - a new mineral of the wodginite group from granitic pegmatites in eastern Kazakhstan. *Mineral. Zh.* **12**, 94–100 (in Russian).

Received January 15, 2018. Revised manuscript accepted June 1, 2018.